Multicomponent Polyanions. 43. A Study of Aqueous Equilibria in the Vanadocitrate System

Per Magnus Ehde, Ingegärd Andersson and Lage Pettersson*

Department of Inorganic Chemistry, University of Umeå, S-901 87 Umeå, Sweden

Ehde, P. M., Andersson, I. and Pettersson, L., 1989. Multicomponent Polyanions. 43. A Study of Aqueous Equilibria in the Vanadocitrate System. – Acta Chem. Scand. 43: 136–143.

The speciation in the H^+-$H_2VO_4^-$-$C_6H_5O_7^{3-}$ system was determined from potentiometric (glass electrode) and ^{51}V NMR measurements. The study was performed in 0.6 M Na(Cl) medium at 25 °C. Due to heavy reduction in acidic solutions, especially with excess citrate, the calculation of emf data had to be restricted to $V/Cit \geq 1.8$ and $-\log[H^+] \geq 3$. Calculations in this range, using the computer program LAKE, indicated the existence of three ternary complexes, $(H^+)_p(H_2VO_4^-)_q(C_6H_5O_7^{3-})_r$, having the (p,q,r) values (1,2,1), (2,2,1) and (3,2,1) with $\log\beta_{1,2,1} = 12.84(5)$, $\log\beta_{2,2,1} = 19.68(2)$ and $\log\beta_{3,2,1} = 24.12(3)$. A tentative structure of a V_2Cit species is proposed and protonation sites are discussed. The NMR data were recorded in the extended region $1 < -\log[H^+] < 8$, including solutions with excess of citrate but freshly prepared so that reduction was negligible. On combining all NMR and emf data at $V/Cit \geq 0.9$, the occurrence of a (3,1,1) complex with $\log\beta_{3,1,1} = 18.1$ was indicated. Moreover, with excess of citrate the NMR spectra showed the existence of an additional minor species, the composition of which could not be determined from the present data set.

In a series of investigations in progress at our department the complexation of V(V) and Mo(VI) with organic oxo ligands is being studied. As V(V) is released to the environment when fossil fuels are burnt and analysis of the vanadium content for instance in trees has revealed an increasing uptake,[1] we have recently focused our attention on V(V) – organic ligand systems. Oxalic acid was first chosen,[2] since it is one of the most abundant organic ligands in nature.[3] As the second example we chose citric acid, CO_2H-CH_2-C(OH)(CO_2H)-CH_2-CO_2H, which is an important metabolic product in all cells and also present in plant leachates[4] and in some soil solutions.[5] Moreover, it forms complexes of similar stability to those of "fulvic acid"[6] and is a potentially tetradentate ligand, which makes the complexation more interesting from a structural viewpoint.

In our previous study of the vanadooxalate system[2] no indication of any ternary complex containing more than one vanadium atom was found. However, Tracey *et al.* have reported binuclear vanadium complexes with methanol[7] and with bi- and tridentate α-hydroxocarboxylic acids[8] as ligands. These complexes are rather weak, and a large excess of the ligand was used. The authors suggest that the oxygen coordination to each vanadium is octahedral, that the two octahedra have one oxygen in common and that the ligands are non-bridging. In a ^1H, ^{13}C and ^{51}V NMR study of vanadium(V) complexes with bi- and tridentate α-hydroxocarboxylic acids, Caldeira *et al.*[9] found that the predominant complexes have a 1:1 composition and "almost certainly in a polymeric structure." One of the ligands studied, the tridentate L-Malic acid, CO_2H-CH_2-CHOH-CO_2H, is structurally related to citric acid. If malic acid forms polynuclear V complexes, citric acid would certainly have the same ability.

Concerning vanadocitrate species, an X-ray structure determination of a V_2Cit_2 compound has been reported.[10] To our knowledge, no equilibrium analysis of the system has been published. The results from the present study are therefore of interest from a physiological and environmental point of view.

Experimental

The present study was carried out in a manner analogous to that in the vanadooxalate study.[2]

Chemicals and analyses. Trisodium citrate dihydrate, $Na_3C_6H_5O_7 \cdot 2H_2O$ (Merck *p.a.*), was dried over concentrated sulfuric acid and used without further purification. The other chemicals used were treated and analysed as described in Refs. 2 and 11. The concentration of H^+-consuming impurities in the titration solutions was found to be $2 \cdot 10^{-5}$ M.

Potentiometric measurements. The measurements were carried out as a series of titrations in 0.6 M Na(Cl) medium at 25 °C. As anion equilibria were being studied, the counterion in the medium, Na^+, was held at a constant concen-

*To whom correspondence should be addressed.

tration. The measurements were made with an automated potentiometric titrator, which has been described in Ref. 12, but subsequently improved. The glass electrodes used were of the general purpose type, Ingold 201-NS. The free hydrogen ion concentration was calculated from the measured emf (in mV) using the equation

$$E = E_o + 59.157 \log[H^+] - 76[H^+]$$

where the last term is the liquid junction potential.

NMR measurements. ^{51}V NMR spectra were recorded at 65.76 MHz (5.9T) using a Bruker WM-250 FT spectrometer. The probe temperature was 24±1 °C throughout. The spectra were obtained from the accumulation of 8000–240000 transients at acquisition times 10^{-1} s. All Free Induction Decays have been multiplied by a line broadening function, LB, of 3 Hz. Due to severe overlapping of peaks, most spectra were also examined under Gaussian resolution enhancement.[13] NMR data were evaluated from computer integrals of peak areas or manually by multiplying the peak height and the half-height width.

Notation. The equilibria studied are written with H^+, $H_2VO_4^-$ and $C_6H_5O_7^{3-}$ as components and thus the complexes are formed according to

$$pH^+ + qH_2VO_4^- + rC_6H_5O_7^{3-} \leftrightarrow$$

$$(H^+)_p(H_2VO_4^-)_q(C_6H_5O_7^{3-})_r.$$

Equilibrium constants are denoted $\beta_{p,q,r}$ and complexes are, for brevity, often given the notation (p,q,r). The symbols *V* and *Cit* stand for the total concentrations of vanadate and citrate, respectively. *H* is the excess concentration of hydrogen ions relative to the zero level (H_2O, $H_2VO_4^-$ and $C_6H_5O_7^{3-}$). The deviation between *H* calculated from potentiometric data, H_{calc}, and *H* calculated from analytical concentrations, H_{tot}, is denoted ΔH. The free concentration of H^+ is denoted *h*.

Computer programs. The mathematical analysis of data was performed with the least-squares program LAKE, a very useful interactive program under development at our department.[14] Included in the program are facilities for selecting data points, total concentration ratios and/or free concentration ranges (e.g. $[H^+]$). Some valuable procedures in the LAKE program are given in Ref. 15. In the present study the analysis of emf data was much simplified and speeded up by the (p,q,r) grid facility. The error squares sum, $U \approx \Sigma(\Delta H)^2$, and the β values for a (p,q,r) combination are first calculated. Then *p* and *q* or *r* are automatically changed a preset number of times by preset increments (usually integers). The *U* values obtained for the different $p(q)_r$ or $p(r)_q$ ranges covered are finally plotted.

In LAKE, the residuals for all the total concentrations are minimized. We have, however, used a weighting factor that gives *H* the predominant contribution to the sum of residuals. The calculations thus become equivalent to LETAGROP calculations.

Table 1. Species and formation constants used in the LAKE calculations [0.6 M Na(Cl), 25 °C].

(*p*, *q*, *r*)	log β_{pqr}	Formula	NMR assignments
1,0,0	–	H^+	–
−1,1,0	−7.92	HVO_4^{2-}	A
0,1,0	–	$H_2VO_4^-$	A
−2,2,0	−15.17	$V_2O_7^{4-}$	B
−1,2,0	−5.25	$HV_2O_7^{3-}$	B
0,2,0	2.77	$H_2V_2O_7^{2-}$	B
−2,4,0	−8.88	$V_4O_{13}^{-6}$	C
−1,4,0	0.22	$HV_4O_{13}^{5-}$	C
0,4,0	10.0	$V_4O_{12}^{4-}$	D
0,5,0	12.4	$V_5O_{15}^{5-}$	E
4,10,0	52.1	$V_{10}O_{28}^{6-}$	F, F^I, F^{II}
5,10,0	58.1	$HV_{10}O_{28}^{5-}$	F, F^I, F^{II}
6,10,0	61.9	$H_2V_{10}O_{28}^{4-}$	F, F^I, F^{II}
7,10,0	63.5	$H_3V_{10}O_{28}^{3-}$	F, F^I, F^{II}
2,1,0	6.96	VO_2^+	G
0,0,1	–	$C_6H_5O_7^{3-}$	–
1,0,1	5.217	$C_6H_6O_7^{2-}$	–
2,0,1	9.298	$C_6H_7O_7^-$	–
3,0,1	12.067	$C_6H_8O_7$	–

The LAKE program has also been used for calculating the percentage of vanadium in different species. Calculation and plotting of distribution and predominance diagrams were performed with the program SOLGASWATER.[16] The computers used were a Cromemco System 300 at our department and a CD Cyber 180-850 at the University Computer Center.

Binary equilibria. The formation constants in the binary H^+-$H_2VO_4^-$ and H^+-$C_6H_5O_7^{3-}$ systems were recalculated from Refs. 11 and 17, since in these references the species HVO_4^{2-} and $C_6H_8O_7$ were chosen as components. The (p,q,r) and $\beta_{p,q,r}$ values are given in Table 1.

Description of data. NMR data. In total, NMR spectra were recorded for 67 vanadocitrate solutions in the ranges $1 < -\log h < 8$, $1 < V/\text{mM} < 36.4$ and $0.025 \leq V/Cit \leq 40$ (Fig. 1). Representative spectra are shown in Figs. 2 and 3. For most solutions the $-\log h$ value was taken from the corresponding potentiometric titration. In some cases, the $-\log h$ value was evaluated from the chemical shift values of the binary vanadate peaks or measured on a calibrated pH-meter, or was calculated from known total concentrations and the final ternary model using SOLGASWATER. In our previous studies on the binary vanadate system[11,18,19] the different peaks were assigned letters, and we have retained that notation (Table 1).

In Fig. 4 the chemical shift values of the ternary peaks 1,

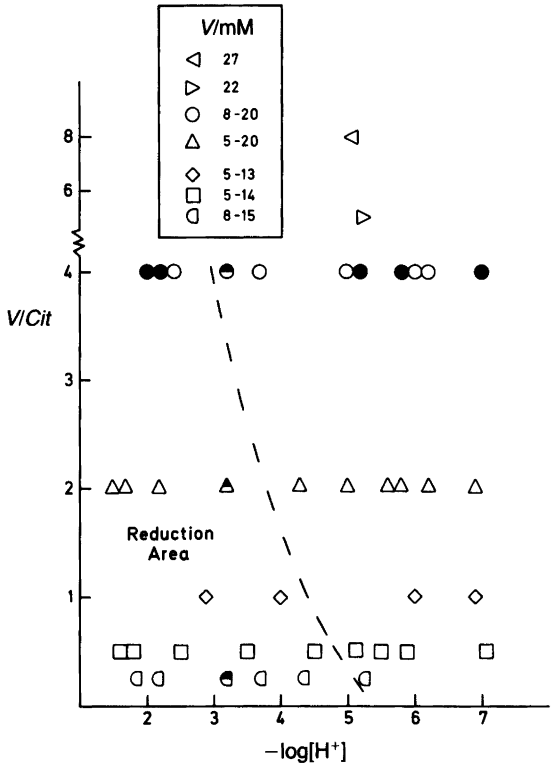

Fig. 1. Points, *V/Cit* (−log[H⁺]), where NMR spectra have been recorded. The filled and half-filled symbols mark the NMR spectra shown in Figs. 2 and 3, respectively.

1′, 1″ and 2 are plotted as a function of $-\log h$. The ternary species first formed on acidification of a neutral vanadocitrate solution give rise to peak 1, which is a single peak even when using high resolution enhancement. At $-\log h \approx 7$ the peak begins to broaden, and on further acidification it splits into two peaks, 1′ and 1″. Below $-\log h = 4$ no $-\log h$ dependence of the chemical shifts is observable. The peaks have equal areas independent of *V/Cit* and $-\log h$. The apparently larger area of 1′ at $-\log h < 2$ results from the VO_2^+ cation, peak G, which has almost the same shift (Fig. 2). At $-\log h \leq 4$ and $V/Cit \leq 1$ a third peak, peak 2, shows up between 1′ and 1″. This peak has no $-\log h$ dependence at all.

Still another peak, denoted peak 3 (not plotted in Fig. 4), is discernible in spectra of solutions at $V/Cit \leq 1$ when $-\log h \leq 6$ (Fig. 3). The chemical shift value is pH-dependent indicating protonation. The present data set shows that the species giving rise to peak 3 never predominates. Even with a four-fold excess of citrate only ≈10 % of the total vanadium concentration is present in the peak 3 species (cf. Table 4). From the present data it is not possible to determine the compositions and formation constants for these species. In the near future we intend to make a complementary study of the system in the region where optimum amounts of the peak 3 species are formed.

All the peaks are fairly broad. The approximate linewidth at half height is $2.6 \cdot 10^2$ Hz for 1, $3.3 \cdot 10^2$ Hz for 1′ and $3.6 \cdot 10^2$ Hz for 1″. Since peak 2 is located between 1′ and 1″, the linewidth could not be evaluated.

Potentiometric data. The present cover the ranges $1 < -\log h < 8.5$, $1 < V/\text{mM} < 40$ and $0.125 \leq V/Cit \leq 40$. A total of 47 titrations were performed and data for 478 experimental points were collected. As reduction of V(V) occurred in slightly acidic solutions even when $V/Cit > 1$, no stable acidic solutions containing both vanadium and citric acid could be prepared. Therefore, neutral vanadocitrate solutions were titrated with HCl. With this procedure it was possible to titrate down to $-\log h \approx 3$ before any observable drift of the emf values occurred. Some titrations at approximately constant $-\log h$ ($-\log h > 5$) and with varied *V/Cit* ratio were also performed. After a thorough inspection of data, more than half of the titration data points had to be excluded due to a slight drift, leaving 244 stable data points that could be used in the calculations.

Analysis of data. The analysis of emf data was carried out in a manner analogous to that in Ref. 2. The ΔH curves indicated a p/q ratio of 1 at high $-\log h$. In the search for the first complex formed, the pH range was restricted to

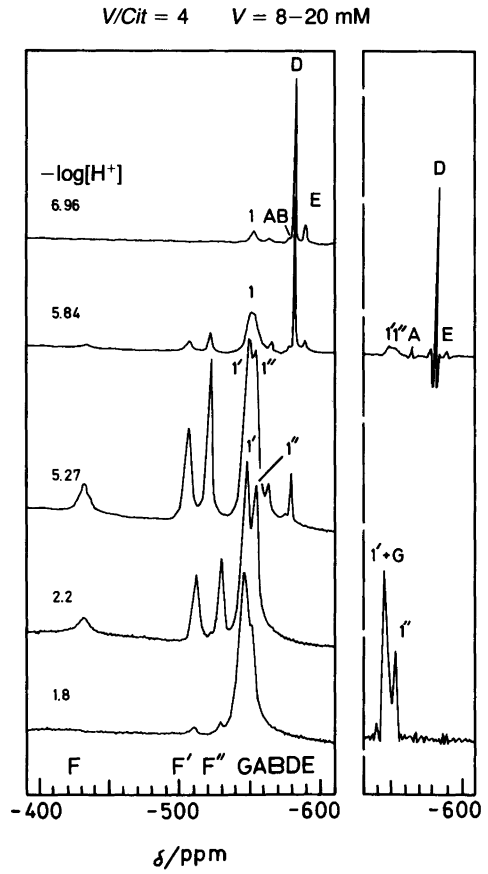

Fig. 2. Some ^{51}V NMR spectra for a −log[H⁺] titration at *V/Cit* = 4. Letters refer to binary vanadates (see Table 1) and figures to ternary species. To the right: spectra with resolution enhancement, *LB* = −400.

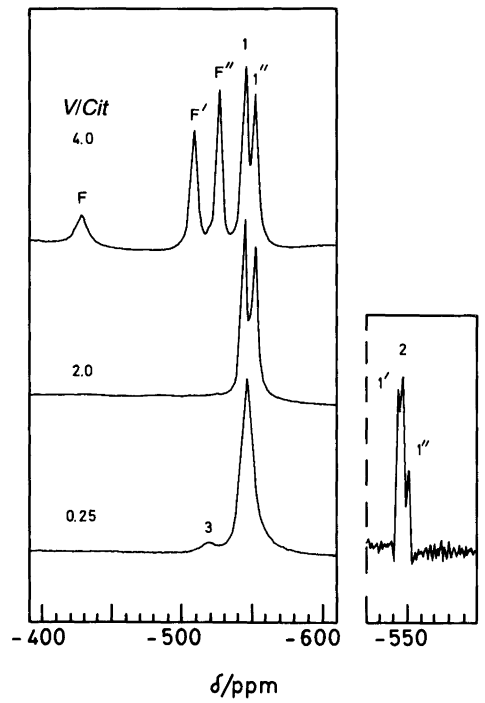

Fig. 3. ^{51}V NMR spectra for solutions with $-\log[H^+] \approx 3.2$ but different *V/Cit* ratios. The total vanadium concentrations are 13.8, 7.40 and 10.4 mM for *V/Cit* = 4, 2 and 0.25, respectively. Letters refer to binary vanadates and figures to ternary species. To the right: spectra with resolution enhancement, *LB* = −500.

$-\log h \geq 6$ (83 titration data points) as the NMR spectra indicated the presence of only one ternary peak in this region. With only binary constants in the model the discrepancy between H_{calc} and H_{tot}, ΔH, was large and the error squares sum, U, was $2256 \cdot 10^{-6}$ M^2. In the (p,q,r) search the lowest U value ($38 \cdot 10^{-6}$ M^2) was obtained for a (2,2,1) species. A (3,3,2) complex gave the next lowest U ($53 \cdot 10^{-6}$ M^2). The U value obtained when (1,2,1) and (2,2,1) were covaried was as low as $1 \cdot 10^{-6}$ M^2 and the

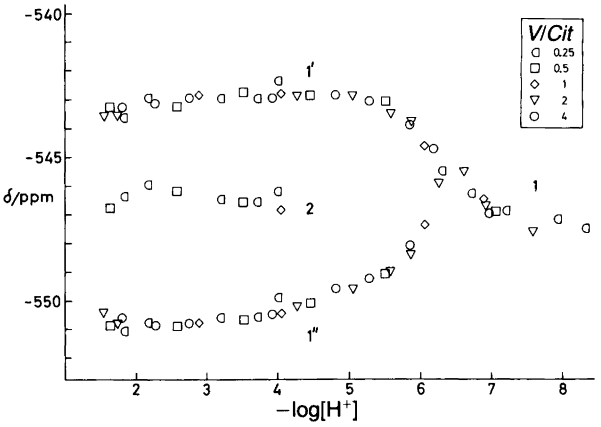

Fig. 4. Chemical shifts, δ, as a function of $-\log[H^+]$ for vanadocitrate species. The shifts for peak 3 have not been included.

remaining residuals were negligible. A dimeric vanadium species is also in accordance with the splitting in more acidic solutions into two NMR peaks, 1′ and 1″, which have equal areas (Figs. 2 and 4). Moreover, the *q/r* ratio of 2 is strongly supported by the fact that the ternary species bind half the vanadium at *V/Cit* = 4 and all the vanadium at *V/Cit* = 2 (Fig. 3).

When the $-\log h$ range in the emf calculations was extended to ≥3 (244 titration data points), (3,2,1) was accepted while (4,2,1) was rejected. The $(p,2,1)$ complexes were from now on considered to be established, and in the continued (p,q,r) search, $\beta_{1,2,1}$ and $\beta_{2,2,1}$ were kept constant while $\beta_{3,2,1}$ was covaried with the new complex(es) tested. Covariation of a constant and simultaneous establishment of a grid in (p,q,r) is another valuable facility of LAKE. The lowest U value was obtained for (3,1,1), viz. $U = 20 \cdot 10^{-6}$ M^2, and the next lowest for (6,2,2), viz. $U = 25 \cdot 10^{-6}$ M^2. Due to the restricted stability range, emf data are thus not very decisive with regard to the species giving rise to peak 2. As (3,1,1) gave a somewhat lower U value and as the species just gives rise to one peak (peak 2), we decided on the monomer. However, some systematic residuals indicated that an additional species was present. A (2,1,1) species was accepted and explained most of the residuals, whereas the next member in the series, (1,1,1), gave such a small contribution that it was excluded. Finally, the (1,2,1), (2,2,1), (3,2,1), (2,1,1) and (3,1,1) complexes were covaried in the range $-\log h \geq 3$ and $V/Cit \geq 0.9$. The last restriction was inserted to minimize the contribution of the peak 3 species. The remaining residuals were small, and it appeared that the speciation was fully established.

The percentage of vanadium bound in different species was then calculated using LAKE. However, when this distribution was compared to the percentages of V obtained from the NMR peak areas, assuming that peaks 1, 1′ and 1″ originate from the $(p,2,1)$ species and peak 2 from the $(p,1,1)$ species, a rather poor fit was obtained in the coexistence region. According to NMR data the $(p,1,1)$ complexes are much weaker and more acidic than indicated from calculations on emf data. The discrepancy may arise from not taking the peak 3 species into account. The $(p,2,1)$ complexes were therefore optimized at $V/Cit \geq 1.8$ and $-\log h \geq 3$ where none of the other ternary species should interfere. The result of this calculation is found in Table 2, Calc. No. 1. The emf residuals were negligible and the formation constants obtained are in full agreement with the experimental NMR data (Table 3). In subsequent calculations these β values were kept constant.

For establishing the peak 2 species the *V/Cit* ratio has to be lowered. We decided to restrict the ratio to $V/Cit \geq 0.9$, since at lower values the contribution from the peak 3 species is not negligible. As expected, the $(p,2,1)$ species could not explain the emf data in the expanded range ($2 > V/Cit > 0.9$). The $\sigma(H)$ value increased by a factor of three (Table 2, Calc. No. 2). In the earlier calculations, when no *V/Cit* restrictions was applied, the lowest U values were obtained for species with $q/r = 1$. Such species were there-

Table 2. Results of the final LAKE calculations. Data for titrations in the range $3 \leq -\log[H^+] \leq 8.2$. The binary constants used are compiled in Tabel 1 [0.6 M Na(Cl), 25 °C]. The error squares sum $U \approx \Sigma(H_{calc} - H_{tot})^2$ is minimized. In calculations Nos. 2–7 the formation constants obtained in calculation No. 1 are kept constant.

Calc. No.	(*p*, *q*, *r*) combination	log $\beta_{p,q,r}$ (3σ)[a]	*V/Cit*	Number of points	$U \cdot 10^7/M^2$	σ(*H*)/mM
1	1,2,1 2,2,1 3,2,1	12.84(5) 19.68(2) 24.12(3)	≥1.8	93	9.3	0.10
2	1,2,1 2,2,1 3,2,1	12.84 19.68 24.12	≥0.9	143	120.1	0.29
3	3,1,1	18.35(7)	≥0.9	143	31.9	0.15
4	2,1,1 3,1,1	14.1(1) 18.41(6)	≥0.9	143	23.4	0.13
5	6,2,2	39,1(1)	≥0.9	143	41.6	0.17
6	4,2,2 5,2,2 6,2,2	31.3(1) 35.3(2) 39.2(1)	≥0.9	143	20.7	0.12
7	3,1,1	18.1[b]	≥0.9	143	52.5	0.19

[a]When no 3σ is given the constant has not been varied. [b]Constant that fits NMR data.

Table 3. Comparison of emf model with NMR data in the (*p*,2,1) range. The emf model used is that of calculation 1 in Table 2.

V/Cit	*V*/mM	$-\log[H^+]$	% V in (*p*,2,1)	
			Exp. NMR data	Emf model
40	36.4	4.9	5	5.0
4	14.8	5.0	50	49.8
4	14.0	3.7	51	49.2
2	18.5	6.9	40	41.6
2	13.3	6.7	58	54.7
2	17.0	6.2	80	79.9
2	16.5	5.9	90	92.0
0.5	13.7	7.1	79	74.7

fore once again thoroughly tested (Calc. Nos. 3–6). The triplet (4,2,2), (5,2,2), (6,2,2) gave a somewhat lower *U* value than the monomeric pair (2,1,1), (3,1,1). It is, however, not likely that three binuclear species would give rise to only one NMR peak, which moreover is not $-\log h$ dependent. We therefore decided on the monomers. Different values for their formation constants were systematically tested until a reasonable fit to the NMR data was obtained. The (2,1,1) species could be excluded, and $\log \beta_{3,1,1} = 18.1$ gave a reasonable fit to both emf data (Calc. No. 7) and NMR data (Table 4). The NMR data are difficult to evaluate quantitatively in the present study and are therefore not of the highest quality. Due to severe overlapping of the peaks 1′, 1″ and 2, resolution enhancement had to be used, which introduced an error in the

Table 4. Comparison of emf model and the combined emf-NMR model with NMR data in the reduction range which means that emf values are not quite reliable. The models used are those of calculation 4 (Emf model) and 7 (Combined model) in Table 2.

V/Cit	*V*/mM	$-\log[H^+]$	% V in (*p*,2,1)			% V in (*p*,1,1)			% V in peak 3
			Exp. NMR data	Emf model	Comb. model	Exp. NMR data	Emf model	Comb. model	Exp. NMR data
1	13.3	4.0	95	93.4	96.7	–	6.6	3.3	5
0.5	9.8	4.5	96	93.9	97.0	–	6.1	3.0	4
0.5	8.5	3.5	79	52.7	78.3	16	47.3	21.7	5
0.5	7.5	2.6	67	30.4	59.7	26	69.2	39.8	8
0.25	14.3	5.0	92	82.8	95.7	1	17.1	4.3	8
0.25	11.1	3.7	72	43.8	74.1	19	56.2	25.9	9
0.25	10.4	3.2	54	27.7	59.4	39	72.3	40.6	7
0.25	9.1	2.2	24	13.5	40.1	64	85.8	58.7	5
0.125	5.0	2.2	25	9.5	33.4	65	89.7	65.2	6

integrals of peak areas. An extreme example of this is shown in Fig. 3. Peak 3 totally disappears when *LB* is changed from 3 to −500 Hz.

Results and discussion

From potentiometric and ^{51}V NMR data we have been able to determine the speciation in the H^+-$H_2VO_4^-$-$C_6H_5O_7^{3-}$ system, although in a somewhat restricted range. The following species and formation constants were obtained: (1,2,1), (2,2,1) and (3,2,1) with $\log\beta_{1,2,1}$ = 12.84(5), $\log\beta_{2,2,1}$ = 19.68(2) and $\log\beta_{3,2,1}$ = 24.12(3). The errors given are 3σ. We are confident that these constants are of high quality, and they agree excellently with NMR data (Table 3). A preliminary analysis of data for the lower *V/Cit* range indicated formation of a (3,1,1) species with $\log\beta_{3,1,1}$ = 18.1. This monomeric species is formed in the reduction range, and the value of the formation constant is mainly based on NMR spectra recorded for freshly prepared solutions.

The vanadocitrate system presents exceptional problems. When *V/Cit* > 2, some of the vanadium is uncomplexed and forms decavanadates. The decavanadates are very slowly decomposed, so that equilibration of these solutions takes up to 24 h. At low *V/Cit* there is spontaneous reduction. In Fig. 1, the area in which reduction takes place is marked; as can be seen, a large part of the complexation region is affected. As the oxidation/reduction process is slow, especially at low total concentrations, and as the equilibria at *V/Cit* ≤ 2 are fast, it has been possible to carry out potentiometric titrations down to $-\log h \approx 3$. The (*p*,2,1) complexes (peaks 1, 1′ and 1″) are very strong, as shown in Fig. 3. At *V/Cit* = 4, half of all vanadium, and at *V/Cit* = 2, practically all vanadium is bound. This means that in order to obtain appreciable amounts of the other ternary species a large excess of citric acid is needed, which on the other hand leads to increased reduction. Moreover, the (3,1,1) complex (peak 2) is acidic and thus hard to evaluate from the restricted emf data range ($-\log h \geq 3$). Without resolution enhancement the existence of the peak 2 species could not have been verified (Fig. 3, lowest spectrum). With enhanced resolution, good shift values for peak 2 can be obtained, but the peak areas are difficult to estimate. Although the presence of the (3,1,1) complex is in accordance with a single NMR peak, the composition of peak 2 cannot be considered firmly established. Furthermore, the species giving rise to the minor peak 3 could not be determined from the present data set and are therefore not included in the emf model.

A good fit between the emf model and the NMR data cannot be achieved with a large excess of citrate, especially in acidic solutions. In Table 2, constants derived in different ways are given. In Table 4, comparisons between the NMR peak areas and different models are made. It is clear that the results obtained in an equilibrium study can be very misleading when using only one experimental method.

The features of Fig. 4 are somewhat peculiar. In the range $8 > -\log h > 7$, peak 1 has approximately the same shift value. At $-\log h \approx 7$ it starts to broaden. Below $-\log h \approx 6$ it splits into two peaks which gradually move apart on acidification. The $-\log h$ dependence of the peaks indicates some sort of exchange, which is fast on the NMR time scale, involving either protons or citrate ligands. Considering our final equilibrium model, Fig. 4 can be explained by the formation of an alkaline complex which has two vanadium atoms with the same chemical environment. An oxygen atom near the vanadium atom which gives rise to peak 1′ is then protonated, which causes broadening and then splitting of peak 1. From the emf calculation we obtained $pK_{2,2,1}$ = 6.84, which is in the $-\log h$ range where the peak broadens. For $-\log h \leq 5.5$ the chemical shift value of peak 1′ becomes constant, while peak 1″ still shows some $-\log h$ dependence. The second proton therefore seems to be located on an oxygen atom adjacent to the vanadium atom giving rise to peak 1″. From emf data, a pK_a of 4.44 was established. The presence of a mononuclear species which dimerizes on acidification could also explain Fig. 4 if the exchange is fast. However, the (*p*,2,1) species fit the emf data so well that no other species were accepted.

To obtain definitive structural information, crystallisation experiments are in progress. We will thereby focus on the (*p*,2,1) species to investigate whether citrate acts as a bridge between two V monomers or stabilizes a binuclear vanadate group. Despite the use of a variety of cations we have so far not obtained crystals of any vanadocitrate species.

A discussion of some structural aspects will however be given, ending up with the proposal of a tentative structure for the V_2Cit species, including possible protonation sites. As four oxygens tetrahedrally coordinated to V give rise to a sharp peak, the broadness of the 1, 1′ and 1″ peaks (≈300 Hz) strongly favours 5 or 6 coordination to oxygen. Distorted octahedral configurations are most frequently found in the vanadoorganic structures published so far. Moreover, these complexes are mononuclear in vanadium and two oxygens are more firmly bonded than the others, forming a VO_2^+ unit. This is valid even with such different ligands as bidentate oxalic acid[20] and tetradentate EDTA.[21] In Fig. 5, a tentative structure of a (*p*,2,1) unit is drawn schematically, based on the assumptions that (i) vanadium is octahedrally coordinated to oxygen, (ii) the two octa-

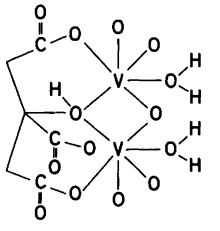

Fig. 5. Schematic structure of a proposed (1, 2, 1) species. The central C atom and the two CH_2 groups are not marked with letters.

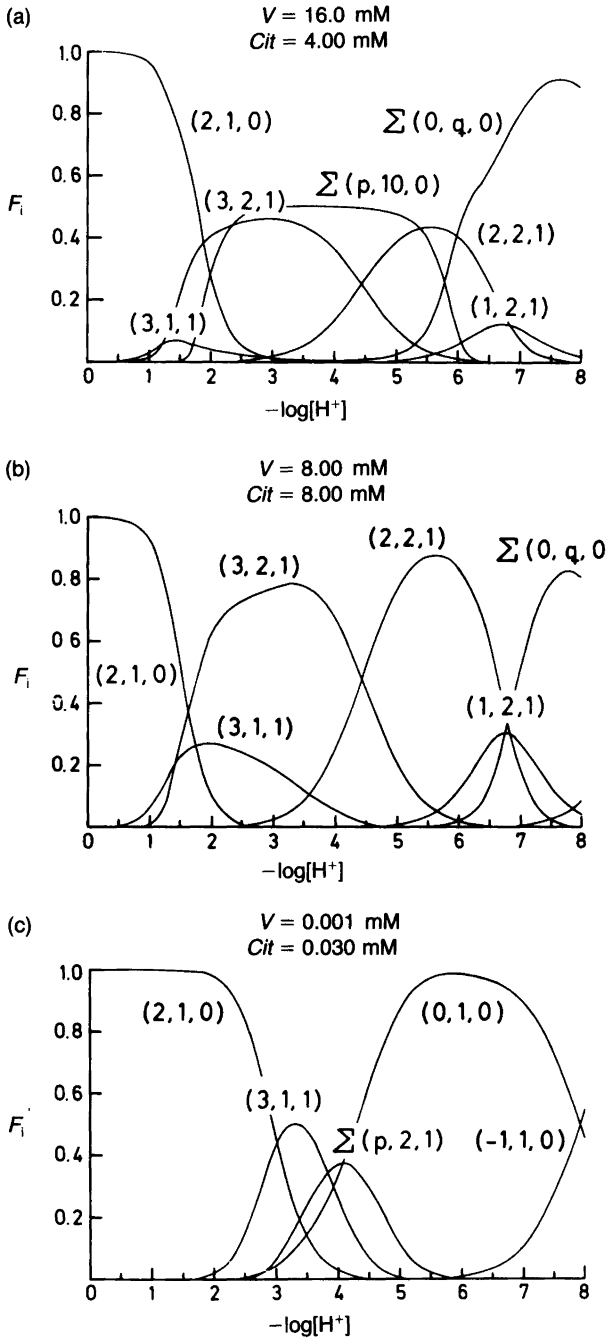

Fig. 6. Diagrams showing the distribution of vanadium in soluble species as a function of $-\log[H^+]$. The quantity F_i is defined as the ratio between vanadium in a species to total vanadium. In the calculations, the constants given in Table 1 and Table 2 (calc. No. 7) were used. Species with $F_i < 0.06$ have been omitted.

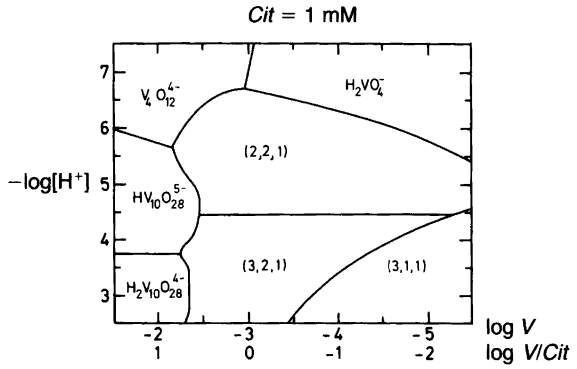

Fig. 7. Diagram showing predominance areas for V-containing species at *Cit* = 1 mM. In each area, the species which has the highest vanadium content is marked.

hedra share an edge, (iii) two oxygens form strong bonds to each V forming a VO_2^+ unit, and (iv) chelate rings with 7 or more atoms are not likely to be formed.

The first (p,2,1) species formed in the system has $p = 1$ and a charge of −4. Five protons attached to oxygen thus have to be added. We have given the most likely positions in Fig. 5. The two V atoms are equivalent and thus give rise to only one NMR signal (peak 1). The most probable protonation site when forming the (2,2,1) complex is the "free" carboxylic group. This would not account for the splitting to 1′ and 1″, unless the −COOH group is hydrogen bonded to a terminal vanadium-bound oxygen in one of the two octahedra. The second protonation probably occurs on the V-O-V oxygen.

Although 6-coordination is to be expected, 5 coordination cannot be excluded. This is easily obtained by removing the water molecule.

The distribution of vanadium in different species is shown in Figs. 6a–c. As the hydrolysis of vanadium(V) is very complex, the diagrams easily become unclear. Therefore, all species that contain less than 6% of the total vanadium concentration have been omitted. Moreover, only the sum of the decavanadate species and the different metavanadate species is shown. Fig. 6a shows the distribution when *V/Cit* = 4. The complexation starts already at $-\log h \approx 8$ and almost half the vanadium is bound in the ternary (p,2,1) complexes in the range $2 < -\log h < 6$. Only at low $-\log h$ is some of the vanadium bound in the (3,1,1) species. When *V/Cit* = 1 (Fig. 6b) no decavanadates are to be found and the ternary species are quite predominant in the range $2.5 < -\log h < 5.5$. The (3,1,1) species has gained in importance but is still a minor species.

The distribution between the (p,2,1) and the (3,1,1) species is dependent on the total vanadium concentration. The monomeric species is favoured by low concentrations. This is exemplified in Fig. 6c, where the distribution has been plotted for V and Cit concentrations which can be found in the environment. Even at such low concentrations, vanadocitrates seem to play an important role in the speciation of vanadium. In Fig. 7 the species that contains most vanadium in an ($-\log h$, $-\log V$) area is marked out. The (p,2,1) species are the predominant ternary species, and only in acid solution, with a large excess of citrate, does (3,1,1) become predominant.

The most interesting finding of the present study is that a polydentate organic oxo-ligand such as citrate can form binuclear vanadium complexes. Although seldom encountered in the current literature, polynuclear species will, in

our opinion, become the rule rather than the exception when systems containing vanadate and organic polydentate oxoligands are studied.

Acknowledgements. We thank Dr. Britt Hedman, Dr. Oliver Howarth and Ann-Marie Nenner, B. Sc. for valuable comments, Ms. Christina Broman for typing the manuscript and Mr. Lage Bodén for drawing the figures. This work forms part of a program supported financially by the Swedish Natural Science Research Council.

References

1. Matusiewicz, H. and Barnes, R. R. *Anal. Chem. 57* (1985) 406.
2. Ehde, P. M., Andersson, I. and Pettersson, L. *Acta Chem. Scand., Ser. A 40* (1986) 489.
3. Steinberg, S. M. and Bada, J. L. *J. Mar. Res. 42* (1984) 697.
4. Muir, J. W., Morrison, R. I., Brown, C. J. and Logan, J. *J. Soil. Sci. 15* (1964) 220.
5. Bruckert, S. *Ann. Agron. 21* (1970) 725.
6. Cressey, P. J., Monk, G. R., Powell, H. K. J. and Tennant, D. J. *J. Soil. Sci. 34* (1983) 783.
7. Tracey, A. S., Gresser, M. J. and Galeffi, B. *Inorg. Chem. 27* (1988) 157.
8. Tracey, A. S., Gresser, M. J. and Parkinson, K. M. *Inorg. Chem. 26* (1987) 629.
9. Caldeira, M. M., Ramos, M. L., Oliveira, N. C. and Gil, V. M. S. *Can. J. Chem. 65* (1987) 2434.
10. Filin, G. I. and Markin, V. N. *Deposited Doc.* (1975) VINITI 162, 3479 (in Russian); *Chem. Abstr. 88* 57252e.
11. Pettersson, L., Hedman, B., Andersson, I. and Ingri, N. *Chem. Scr. 22* (1983) 254.
12. Ginstrup, O. *Chem. Instrum. 4* (1973) 141.
13. Lyndon, J. C. and Ferrige, A. G. *Prog. NMR Spectrosc. 14* (1980) 27.
14. Holmström, K. *Thesis,* Umeå University, Umeå, Sweden 1988.
15. Yagasaki, A., Andersson, I. and Pettersson, L. *Inorg. Chem. 26* (1987) 3926.
16. Eriksson, G. *Anal. Chim. Acta 112* (1979) 375.
17. Öhman, L.-O. and Sjöberg, S. *J. Chem. Soc., Dalton Trans.* (1983) 2513.
18. Pettersson, L., Hedman, B., Nenner, A.-M. and Andersson, I. *Acta Chem. Scand., Ser. A 39* (1985) 499.
19. Pettersson, L., Andersson, I. and Hedman, B. *Chem. Scr. 25* (1985) 309.
20. Drew, R. E., Einstein, F. W. B. and Gransden, S. E. *Can. J. Chem. 52* (1974) 2184.
21. Scheidt, W. R., Collins, D. M. and Hoard, J. L. *J. Am. Chem. Soc. 93* (1971) 3873.

Received April 12, 1988.